

Influence of inclined magnetic field and heat transfer on peristaltic transfer Powell-Eyring fluid in asymmetric channel and porous medium

Ali Khalefa Hage*, Liqaa Zeki Hummady

Department of Mathematic, University of Baghdad, Baghdad, Iraq

(Communicated by Mohammad Bagher Ghaemi)

Abstract

Peristaltic motion of a magnetohydrodynamic Powell-Eyring fluid in an asymmetric channel with porous walls. medium is investigated in the present study. The modeling of Mathematic is created in the presence of a stable inclined magnetic field and the angle with the vertical axis can be made, using constitutive equations following the Powell-Eyring fluid model. In flow analysis, assumptions such as long wave length approximation and low Reynolds number are utilized. Closed form formulas for the stream function and mechanical efficiency are created. On the channel walls, pressure rise per wave length has been calculated numerically. The effects of the Hartman number (Ha), Darcy number (Da), material fluid (A), inclination of magnetic field (β), porous media parameter (w), amplitude ratio (θ), pumpinh, The effects of the magnetic field's inclination on axial velocity and entrapment are investigated in detail and graphically shown.

Keywords: Inclined magnetic field, Powell-Eyring, peristaltic flow and heat transfer
2020 MSC: Primary 90C33, Secondary 26B25

1 Introduction

The Peristalsis is a phenomenon in which fluid movement occurs as a series of Waves of contraction, or expansion travel down a distensible tube's length [3]. Food movement in the intestines, lymphatic blood flow, the passage of urine from kidney straight to the bladder, and blood flow in tiny arteries are all physiological processed, that can be identified. It is also used in biomedical engineering, chemical processes, medicine, and worm movement are completed by Latham [11], and Shapiro et al. [13] using other experimental and theoretical methods. The introduction of non-Newtonian fluids in these applications is an important observation that can be taken from the application mentioned above. Polymer melts, blood, fruit juices, ceramics, and multigrade oil belong to the Non-Newtonian Fluids, are also examples and a lot others [4]. Shear stress and rate of deformation's relationship can be described using its own "constitutive equation". The Powell-Eyring model is preferred over other non-Newtonian fluid models because it is derived from the kinetic of liquids theory rather than an empirical relationship. It accurately reduces to Newtonian behavior for high and low shear rates. The term "peristaltic transport" and "Non-Newtonian fluid" were used by many scholars as a title for their

*Corresponding author

Email addresses: ali.khalifa1203a@sc.uobaghdad.edu.iq (Ali Khalefa Hage), liqaa.hummady@sc.uobaghdad.edu.iq (Liqaa Zeki Hummady)

papers to achieve this goal (see [8, 10, 12]). When a magnetic field is supplied to move a conducting fluid, it induces an electromagnetic field, which causes the Lorentz force, that acts in the opposite direction of the fluid motion. Peristaltic flow is used in various applications and activities, including blood pumping devices, therapy of cancer, Magnetic resonance imaging (MRI) for brain diagnostics, biomedical engineering, industries, power generators, electrostatic precipitation, and geophysics are among the other disciplines. . Regarding the various scenarios, the investigations attempted to link peristaltic flow under the influence of magnetic fluid [8, 12, 15]. Transport through porous media, on the other hand, is beneficial and practical in a range of sectors. , including geomechanics, biomechanics, industry, fluid filtration, seepage of water in riverbeds, and human lung function, among others. Many researchers were prompted by these applications to look into the combined effect of a porous media and a magnetic field on fluid flows in various geometries and conditions (see [2, 5]) . Many applications, such as the industry of current material (polymer industry) produces microscopic wall slips for technical and medicinal applications (polishing artificial heart), and technical process, rely heavily on slip conditions rather than no-slip conditions. The influence of slip circumstances on peristaltic flow of non-Newtonian fluids was examined in the aforementioned application described through investigations [7]. The impact of heat and mass transfer on peristaltic flow for MHD Powell-Eyring fluid with slip condition has begun to be discussed [6]. The influence of slip condition on Eyring-Powell fluid peristaltic flow was investigated [10]. Veerakrishna, et al. Peristaltic flow in an inclined symmetric channel with slip condition: heat transfer , Williamson fluid model was discovered [1]. In a non-uniform porous channel, explore the immediate effects of slip and MHD on peristaltic blood flow using the Jeffery fluid model. Tanveer et al. [14]. The effect of an angled magnetic field on Powell-Eyring fluid peristaltic transport in a conduit with flexible walls is investigated. The goal of this research is to look at the impact of a magnetic field and a porous media on the peristaltic transient of a Non-Newtonian fluid in an asymmetric channel with shear stress-dependent slip. The Powell-Eyring fluid model governs non-Newtonian fluids. The research is carried out under the use of a long wavelength and a low Renold number as a starting point. The wave frame was used to develop the flow's governing equation. The determination of Closed expressions for stream function, velocity axial, and pressure gradient was made, as well as numerical integration of pressure rise for each unit wave using series approximation. Finally, a graphical analysis was performed to determine.

2 Mathematical Formulation for Asymmetric Flow

Considering the flow of a Powell-Eyring fluid in a two-dimensional asymmetric, channel has width $(d + d')$. The flow is created by an infinite sinusoidal wave line traveling forth with constant velocity c along on the channel's walls. Asymmetric channels are created by altering wave amplitudes, phase angles, and channel widths. The geometries of the walls are modeled as

$$\bar{h}_1(\bar{x}, \bar{t}) = d - a_1 \sin \left[\frac{2\pi}{\lambda} (\bar{x} - c\bar{t}) \right] \text{ upper wall,} \quad (2.1)$$

$$\bar{h}_2(\bar{x}, \bar{t}) = -d' - a_2 \sin \left[\frac{2\pi}{\lambda} (\bar{x} - c\bar{t}) + \emptyset \right] \text{ lower wall.} \quad (2.2)$$

where $a_1, a_2, d, d', \lambda, c, \emptyset, t$, are the wave's' amplitudes, channels' width, wavelength, and the speed of wave, $(0 \leq \emptyset \leq \pi)$. The rectangular coordinating system and phase difference are chosen. So that the, X.-axis is parallel to the axis of X.-axis and the, Y.-axis is perpendicular to the axis of,X.-axis. It's worth noting that $(\emptyset = 0)$ denotes a symmetric channel with out-of-phase waves, whereas $(\emptyset = \pi)$ denotes in-phase waves. Furthermore, a_1, a_2, d, d' .and meet the condition. :

$$a_1^2 + a_2^2 + 2a_1 a_2 \cos(\emptyset) \leq (d + d')^2$$

As assumed, there is no longitudinal walls' motion. This assumption limits wall deformation ,However, this does not mean that the channel is rigid while moving longitudinally.

3 Basic Equation

The fluid follows the Powell Erring model, and the Cauchy stress tensor,. of it is as follows [14]:

$$\bar{\tau} = -PI + \bar{S}, \quad (3.1)$$

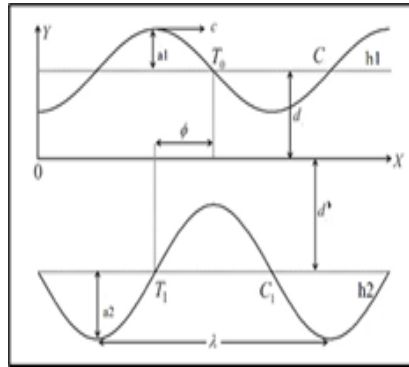


Figure 1: Cartesian Dimensional Asymmetric Channels Coordinates.

$$\bar{S} = \left[\mu + \frac{1}{\beta \dot{\gamma}} \sinh^{-1} \left(\frac{\dot{\gamma}}{c_1} \right) \right] A_{11}, \quad (3.2)$$

$$\dot{\gamma} = \sqrt{\frac{1}{2} \text{tr}(A_{11})^2}, \quad (3.3)$$

$$A_{11} = \nabla \bar{V} + (\nabla \bar{V})^T. \quad (3.4)$$

where (\bar{S}) expresses the extra tensor's stress, I the identity tensor, $\bar{\nabla} = (\partial \bar{X}, \partial \bar{Y}, 0)$ the gradient vector, (β, c_1) the Powell-Eyring fluid's material characteristics, (\bar{P}) the fluid's pressure, and (μ) the dynamic viscosity.

The terms \sinh^{-1} is approximated as

$$\sinh^{-1} \left(\frac{\dot{\gamma}}{c_1} \right) = \frac{\dot{\gamma}}{c_1} - \frac{\dot{\gamma}^3}{6c_1^3} + \frac{\dot{\gamma}^5}{c_1^5} \ll 1. \quad (3.5)$$

$$\bar{s}_{\bar{x}\bar{x}} = 2 \left(\mu + \frac{1}{\beta c_1} \right) \bar{u}_{\bar{x}} - \frac{1}{3\beta c_1^3} \left[2\bar{u}_{\bar{x}}^2 + (\bar{v}_{\bar{x}} + \bar{u}_{\bar{y}})^2 + 2\bar{v}_{\bar{y}}^2 \right] \bar{u}_{\bar{x}}, \quad (3.6)$$

$$\bar{s}_{\bar{x}\bar{y}} = \left(\mu + \frac{1}{\beta c_1} \right) (\bar{v}_{\bar{x}} + \bar{u}_{\bar{y}}) - \frac{1}{6\beta c_1^3} \left[2\bar{u}_{\bar{x}}^2 + (\bar{v}_{\bar{x}} + \bar{u}_{\bar{y}})^2 + 2\bar{v}_{\bar{y}}^2 \right] (\bar{v}_{\bar{x}} + \bar{u}_{\bar{y}}), \quad (3.7)$$

and

$$\bar{s}_{\bar{y}\bar{y}} = 2 \left(\mu + \frac{1}{\beta c_1} \right) \bar{v}_{\bar{y}} - \frac{1}{3\beta c_1^3} \left[2\bar{u}_{\bar{x}}^2 + (\bar{v}_{\bar{x}} + \bar{u}_{\bar{y}})^2 + 2\bar{v}_{\bar{y}}^2 \right] \bar{v}_{\bar{y}}. \quad (3.8)$$

4 The governing equation

In the laboratory frame (\bar{x}, \bar{y}) , the dominated equations of motion in an inclined channel with inclined magnetic field of Powell-Eyring fluid can be written as the continuous equation:

$$\frac{\partial \bar{u}}{\partial \bar{x}} + \frac{\partial \bar{v}}{\partial \bar{y}} = 0. \quad (4.1)$$

The \bar{x} -component of moment equation:

$$\rho \left(\frac{\partial \bar{u}}{\partial t} + \bar{u} \frac{\partial \bar{u}}{\partial \bar{x}} + \bar{v} \frac{\partial \bar{u}}{\partial \bar{y}} \right) = - \frac{\partial \bar{p}}{\partial \bar{x}} + \frac{\partial}{\partial \bar{x}} \bar{s}_{\bar{x}\bar{x}} + \frac{\partial}{\partial \bar{y}} \bar{s}_{\bar{x}\bar{y}} - \sigma \beta_0^2 \cos \beta (\bar{u} \cos \beta - \bar{v} \sin \beta) - \frac{\mu}{k} \bar{u}. \quad (4.2)$$

The \bar{y} - component of moment equation :

$$\rho \left(\frac{\partial \bar{v}}{\partial \bar{t}} + \bar{u} \frac{\partial \bar{v}}{\partial \bar{x}} + \bar{v} \frac{\partial \bar{v}}{\partial \bar{y}} \right) = - \frac{\partial \bar{p}}{\partial \bar{y}} + \frac{\partial}{\partial \bar{x}} \bar{s}_{x\bar{y}} + \frac{\partial}{\partial \bar{y}} \bar{s}_{y\bar{y}} - \sigma \beta_0^2 \sin \beta (\bar{u} \cos \beta - \bar{v} \sin \beta) - \frac{\mu}{\bar{k}} \bar{v}. \tag{4.3}$$

The energy equation:

$$\rho c_p \left(\frac{\partial}{\partial \bar{t}} + \bar{u} \frac{\partial}{\partial \bar{x}} + \bar{v} \frac{\partial}{\partial \bar{y}} \right) \bar{T} = k' \left(\frac{\partial^2}{\partial \bar{t}^2} + \frac{\partial^2}{\partial \bar{x}^2} + \frac{\partial^2}{\partial \bar{y}^2} \right) \bar{T} + \mu \left[\left(\frac{\partial \bar{u}}{\partial \bar{y}} + \frac{\partial \bar{v}}{\partial \bar{x}} \right)^2 + 2 \left(\frac{\partial \bar{u}}{\partial \bar{x}} \right)^2 + 2 \left(\frac{\partial \bar{v}}{\partial \bar{y}} \right)^2 \right] \tag{4.4}$$

where the $\rho, \bar{u}, \bar{v}, \bar{y}, \bar{p}, \mu, \bar{k}, B_0$ are the density of fluid. The conductivity of electricity is axisymmetric pressure, viscosity, material constant, permeability parameter, and constant magnetic field are all terms that can be used to describe velocity, transverse velocity, transverse coordinate, pressure, viscosity, material constant, permeability parameter, and constant magnetic field. are all terms that can be used to describe pressure, viscosity, material constant, permeability parameter, and constant magnetic field axial velocity, transverse velocity, transverse coordinate, pressure, viscosity, material constant, permeability parameter, and constant magnetic field.

In the laboratory frame (\bar{x}, \bar{y}) , the flow is unstable, but steady in a coordinate system traveling at the speed of the wave (c) in the wave's frame (\bar{x}, \bar{y}) .

The following non-dimensional quantities were set up, to carry out the non-dimensional analysis:

$$\begin{aligned} x &= \frac{1}{\lambda} \bar{x}, y = \frac{1}{d} \bar{y}, u = \frac{1}{c} \bar{u}, \quad v = \frac{1}{\delta c} \bar{v}, p = \frac{d^2}{\lambda \mu c} \bar{p}, t = \frac{c}{\lambda} \bar{t}, h_1 = \frac{1}{d} \bar{h}_1, h_2 = \frac{1}{d} \bar{h}_2, \delta = \frac{d}{\lambda}, \theta = \frac{b}{d}, \\ \text{Re} &= \frac{\rho c d}{\mu}, \text{Ha} = d \sqrt{\frac{\sigma}{\mu}} \beta_0, \text{Da} = \frac{\bar{k}}{d^2}, w = \frac{1}{\mu \beta c_1}, \quad A = \frac{w}{6} \left(\frac{c}{c_1 d} \right)^2, \bar{T} = T - T_0, \theta = \frac{T - T_0}{T_1 - T_0}, \\ Ec &= \frac{c^2}{c_p (T_1 - T_0)}, \text{Pr} = \frac{\mu c_p}{k'}, \quad s_{xx} = \frac{\lambda}{\mu c} \bar{s}_{x\bar{x}}, s_{xy} = \frac{d}{\mu c} \bar{s}_{x\bar{y}}, \quad s_{yy} = \frac{d}{\mu c} \bar{s}_{y\bar{y}}. \end{aligned} \tag{4.5}$$

(w) is the dimensionless permeability of the porous medium parameter, (Re) is the Renold number, (Ha) is the Hartman number, (θ) is the amplitude ratio, (Da) and (A) are material fluid parameters.

Then, in view of Eq. (4.5), Eq. (2.1), (2.2), and (3.6) to (4.4) take the form:

The equation (2.1) becomes:

$$h_1(x, t) = 1 - a \sin X. \tag{4.6}$$

The equation (2.2) becomes:

$$h_2(x, t) = -d^* - b \sin[X + \theta]. \tag{4.7}$$

The equation (3.6) becomes :

$$s_{xx} = 2(1 + w) \frac{\partial u}{\partial x} - 2 A \left[2\delta^2 \left(\frac{\partial u}{\partial x} \right)^2 + \left(\delta^2 \frac{\partial v}{\partial x} + \frac{\partial u}{\partial y} \right)^2 + 2\delta^2 \left(\frac{\partial v}{\partial y} \right)^2 \right] \frac{\partial u}{\partial x}. \tag{4.8}$$

The equation (3.7) becomes:

$$s_{xy} = (1 + w) \left(\delta^2 \frac{\partial v}{\partial x} + \frac{\partial u}{\partial y} \right) - A \left[2\delta^2 \left(\frac{\partial u}{\partial x} \right)^2 + \left(\delta^2 \frac{\partial v}{\partial x} + \frac{\partial u}{\partial y} \right)^2 + 2\delta^2 \left(\frac{\partial v}{\partial y} \right)^2 \right] \left(\delta^2 \frac{\partial v}{\partial x} + \frac{\partial u}{\partial y} \right). \tag{4.9}$$

The equation (3.8) becomes:

$$s_{yy} = 2(1 + w) \delta \frac{\partial v}{\partial y} - 2 A \delta \left[2\delta^2 \left(\frac{\partial u}{\partial x} \right)^2 + \left(\delta^2 \frac{\partial v}{\partial x} + \frac{\partial u}{\partial y} \right)^2 + 2\delta^2 \left(\frac{\partial v}{\partial y} \right)^2 \right] \frac{\partial v}{\partial y}. \tag{4.10}$$

The equation (4.1) becomes:

$$\frac{\partial u}{\partial x} + \frac{\partial v}{\partial y} = 0. \tag{4.11}$$

The equation (4.2) becomes

$$\text{Re } \delta \left(\frac{\partial u}{\partial t} + u \frac{\partial u}{\partial x} + v \frac{\partial u}{\partial y} \right) = -\frac{\partial p}{\partial x} + \delta^2 \frac{\partial}{\partial x} s_{xx} + \frac{\partial}{\partial y} s_{xy} - \text{Ha}^2 \cos \beta (u \cos \beta - \delta v \sin \beta) - \frac{1}{\text{Da}} u \tag{4.12}$$

and then Eq. (4.3) becomes

$$\text{Re } \delta^3 \left(\frac{\partial v}{\partial t} + u \frac{\partial v}{\partial x} + v \frac{\partial v}{\partial y} \right) = -\frac{\partial p}{\partial y} + \delta^2 \frac{\partial}{\partial x} s_{xy} + \delta \frac{\partial}{\partial y} s_{yy} + \text{Ha}^2 \sin \beta (\delta u \cos \beta - \delta^2 v \sin \beta) - \delta^2 \frac{v}{\text{Da}}. \tag{4.13}$$

The Energy equation (4.4) becomes:

$$\begin{aligned} \text{Re } \delta \left(\frac{\partial}{\partial t} + u \frac{\partial}{\partial x} + v \frac{\partial}{\partial y} \right) \theta &= \frac{1}{\text{Pr}} \left(c^2 \delta^2 \frac{\partial^2}{\partial t^2} + \delta^2 \frac{\partial^2}{\partial x^2} + \frac{\partial^2}{\partial y^2} \right) \theta \\ &+ \text{Ec} \left[\left(\frac{\partial u}{\partial y} + \delta^2 \frac{\partial v}{\partial x} \right)^2 + 2\delta^2 \left(\frac{\partial u}{\partial x} \right)^2 + 2\delta^2 \left(\frac{\partial v}{\partial y} \right)^2 \right]. \end{aligned} \tag{4.14}$$

The next relationships connect the stream function (Ψ) to the velocity components:

$$u = \frac{\partial \Psi}{\partial y}, v = -\frac{\partial \Psi}{\partial x}. \tag{4.15}$$

Substituted Eqs.(4.15) in Eqs. (4.8), (4.9), (4.10), (4.11), (4.12), (4.13) and (4.14) respectively

$$s_{xx} = 2(1+w) \frac{\partial^2 \Psi}{\partial x \partial y} - 2A \left[2\delta^2 \left(\frac{\partial^2 \Psi}{\partial x \partial y} \right)^2 + \left(-\delta^2 \frac{\partial^2 \Psi}{\partial x^2} + \frac{\partial^2 \Psi}{\partial y^2} \right)^2 + 2\delta^2 \left(-\frac{\partial^2 \Psi}{\partial x \partial y} \right)^2 \right] \frac{\partial^2 \Psi}{\partial x \partial y}, \tag{4.16}$$

$$\begin{aligned} s_{xy} &= (1+w) \left(-\delta^2 \frac{\partial^2 \Psi}{\partial x^2} + \frac{\partial^2 \Psi}{\partial y^2} \right) - \\ &2A \left[2\delta^2 \left(\frac{\partial^2 \Psi}{\partial x \partial y} \right)^2 + \left(-\delta^2 \frac{\partial^2 \Psi}{\partial x^2} + \frac{\partial^2 \Psi}{\partial y^2} \right)^2 + 2\delta^2 \left(-\frac{\partial^2 \Psi}{\partial x \partial y} \right)^2 \right] \left(-\delta^2 \frac{\partial^2 \Psi}{\partial x^2} + \frac{\partial^2 \Psi}{\partial y^2} \right), \end{aligned} \tag{4.17}$$

$$s_{yy} = -2(1+w)\delta \frac{\partial^2 \Psi}{\partial x \partial y} - 2A\delta \left[2\delta^2 \left(\frac{\partial^2 \Psi}{\partial x \partial y} \right)^2 + \left(-\delta^2 \frac{\partial^2 \Psi}{\partial x^2} + \frac{\partial^2 \Psi}{\partial y^2} \right)^2 + 2\delta^2 \left(-\frac{\partial^2 \Psi}{\partial x \partial y} \right)^2 \right] \frac{\partial^2 \Psi}{\partial x \partial y}, \tag{4.18}$$

$$\frac{\partial^2 \Psi}{\partial x \partial y} - \frac{\partial^2 \Psi}{\partial x \partial y} = 0, \tag{4.19}$$

$$\begin{aligned} \text{Re } \delta \left(\frac{\partial^2 \Psi}{\partial t \partial y} + \frac{\partial^3 \Psi}{\partial x \partial y^2} - \frac{\partial^3 \Psi}{\partial x \partial y^2} \right) &= -\frac{\partial p}{\partial x} + \delta^2 \frac{\partial}{\partial x} s_{xx} + \frac{\partial}{\partial y} s_{xy} - \text{Ha}^2 \cos \beta \left(\frac{\partial \Psi}{\partial y} \cos \beta + \delta \frac{\partial \Psi}{\partial x} \sin \beta \right) \\ &- \frac{1}{\text{Da}} \frac{\partial \Psi}{\partial y}, \end{aligned} \tag{4.20}$$

$$\begin{aligned} \text{Re } \delta^3 \left(-\frac{\partial^2 \Psi}{\partial t \partial y} + \frac{\partial^3 \Psi}{\partial x^2 \partial y} - \frac{\partial^3 \Psi}{\partial x^2 \partial y} \right) &= -\frac{\partial p}{\partial y} + \delta^2 \frac{\partial}{\partial x} s_{xy} + \delta \frac{\partial}{\partial y} s_{yy} + \text{Ha}^2 \sin \beta \left(\delta \frac{\partial \Psi}{\partial y} \cos \beta + \delta^2 \frac{\partial \Psi}{\partial x} \sin \beta \right) \\ &+ \delta^2 \frac{1}{\text{Da}} \frac{\partial \Psi}{\partial x} \end{aligned} \tag{4.21}$$

$$\begin{aligned} \text{Re } \delta \left(\frac{\partial}{\partial t} + \frac{\partial^2 \Psi}{\partial x \partial y} - \frac{\partial^2 \Psi}{\partial x \partial y} \right) \theta &= \frac{1}{\text{Pr}} \left(c^2 \delta^2 \frac{\partial^2}{\partial t^2} + \delta^2 \frac{\partial^2}{\partial x^2} + \frac{\partial^2}{\partial y^2} \right) \theta \\ &+ \text{Ec} \left[\left(\frac{\partial^2 \Psi}{\partial y^2} - \delta^2 \frac{\partial^2 \Psi}{\partial x^2} \right)^2 + 2\delta^2 \left(\frac{\partial^2 \Psi}{\partial x \partial y} \right)^2 - 2\delta^2 \left(\frac{\partial^2 \Psi}{\partial x \partial y} \right)^2 \right]. \end{aligned} \tag{4.22}$$

In the wave frame, the dimensionless boundary conditions are [9] :

$$\Psi = \frac{F}{2}, \frac{\partial \Psi}{\partial y} = -1 \text{ at } y = h_1 \tag{4.23}$$

$$\Psi = -\frac{F}{2}, \frac{\partial \Psi}{\partial y} = -1 \text{ at } y = h_2 \tag{4.24}$$

5 The problem’s Solution

Because Eq.(4.22) is highly nonlinear and difficult, obtaining for all of the arbitrary parameters, a closed form solution involved is impossible. To locate the solution, we use the perturbation approach. We extend for the perturbation solution .

$$\begin{aligned} \Psi &= \Psi_0 + A\Psi_1 + O(A^2) \\ F &= F_0 + AF_1 + O(A^2) \\ p &= p_0 + Ap_1 + O(A^2) \end{aligned} \tag{5.1}$$

Substitute the terms (5.1) into Eqs. (4.16)-(4.22), together with the boundary conditions Eqs. (4.23) and (4.24) Since $\delta \leq 1$, the higher terms of order involve the power of δ which are smaller and hence unimportant, we get the following system of equations by equating the coefficients of comparable powers of A :

From Eq. (4.17) and Eq. (4.20) we get :

$$\frac{\partial p}{\partial x} = \Psi_{yyy} - \eta A \frac{\partial}{\partial y} \Psi_{yy}^3 - \xi \Psi_y \tag{5.2}$$

$$\xi = \frac{Ha^2 \cos^2 \beta + \frac{1}{Da}}{w + 1} \tag{5.3}$$

$$\eta = \frac{1}{w + 1} \tag{5.4}$$

from differential of y for Eq (5.2)

$$0 = \Psi_{yyyy} - \eta A \frac{\partial^2}{\partial y^2} \Psi_{yy}^3 - \xi \Psi_{yy} \tag{5.5}$$

From Eq. (4.21) we get :

$$\frac{\partial p}{\partial y} = 0 \tag{5.6}$$

From Eq. (4.22) we get :

$$\theta_{yy} = -Ec \cdot Pr (\Psi_{yy})^2 \tag{5.7}$$

5.1 Zero order system

When the terms of order (A) are negligible in the zeroth order system, we get:

$$\Psi_{0yyyy} - \xi \Psi_{0yy} = 0. \tag{5.8}$$

Such that

$$\begin{aligned} \Psi_0 &= \frac{F_0}{2}, \frac{\partial \Psi_0}{\partial y} = -1 \text{ at } y = h_1 \text{ and} \\ \Psi_0 &= -\frac{F_0}{2}, \frac{\partial \Psi_0}{\partial y} = -1 \text{ at } y = h_2. \end{aligned} \tag{5.9}$$

5.2 First order system

$$\Psi_{1_{yyyy}} - \eta \frac{\partial^2}{\partial y^2} \Psi_{0_{yy}}^3 - \xi \Psi_{1_{yy}} = 0 \tag{5.10}$$

$$\Psi_{1_{yyyy}} - \xi \Psi_{1_{yy}} = \eta \frac{\partial^2}{\partial y^2} \Psi_{0_{yy}}^3 \tag{5.11}$$

$$\Psi_1 = \frac{F_1}{2}, \frac{\partial \Psi_1}{\partial y} = -1 \text{ at } y = h_1 \text{ and } \Psi_1 = -\frac{F_1}{2}, \frac{\partial \Psi_1}{\partial y} = -1 \text{ at } y = h_2 \tag{5.12}$$

We get the final equation for stream function by solving the associated zeroth and first order systems:

$$\Psi = \Psi_0 + A\Psi_1 \tag{5.13}$$

$$\begin{aligned} \Psi = & \frac{e^{-y\sqrt{\zeta}} (e^{2y\sqrt{\zeta}}c_1 + c_2)}{\zeta} + c_3 + y * c_4 + A \left[\left(e^{-3y\sqrt{\zeta}} \left(-e^{6y\sqrt{\zeta}}(h_1 - h_2)^3(-1 + \sqrt{\zeta})^3\zeta^3\eta - \right. \right. \right. \\ & e^{3(h_1+h_2)\sqrt{\zeta}}(h_1 - h_2)^3(1 + \sqrt{\zeta})^3\zeta^3\eta - 6e^{(h_1+h_2+4y)\sqrt{\zeta}}(h_1 - h_2)^3(-1 + \sqrt{\zeta})^2(1 + \sqrt{\zeta})(-5+ \\ & 2y\sqrt{\zeta})\zeta^3\eta + 6e^{2(h_1+h_2+y)\sqrt{\zeta}}(h_1 - h_2)^3(-1 + \sqrt{\zeta})(1 + \sqrt{\zeta})^2(5 + 2y\sqrt{\zeta})\zeta^3\eta + \\ & 8e^{(3h_1+4y)\sqrt{\zeta}}(-2 + h_1(-1 + \zeta)\sqrt{\zeta} - h_2(-1 + \zeta)\sqrt{\zeta})^3 A_1 + 8e^{(3h_1+4y)\sqrt{\zeta}}(2 + h_1(-1 + \zeta)\sqrt{\zeta} - \\ & h_2(-1 + \zeta)\sqrt{\zeta})^3 A_1 + 24e^{(h_1+2h_2+4y)\sqrt{\zeta}}(2 + h_1(-1 + \zeta)\sqrt{\zeta} - h_2(-1 + \zeta)\sqrt{\zeta})(2 - h_1(-1 + \\ & \zeta)\sqrt{\zeta} + h_2(-1 + \zeta)\sqrt{\zeta})^2 A_1 + 8e^{(3h_2+2y)\sqrt{\zeta}}(-2 + h_1(-1 + \zeta)\sqrt{\zeta} - h_2(-1 + \zeta)\sqrt{\zeta})^3 A_2 + \\ & 24e^{(2h_1+h_2+2y)\sqrt{\zeta}}(-2 + h_1(-1 + \zeta)\sqrt{\zeta} - h_2(-1 + \zeta)\sqrt{\zeta})(2 + h_1(-1 + \zeta)\sqrt{\zeta} - h_2(-1 + \\ & \zeta)\sqrt{\zeta})^2 A_2 + 8e^{(3h_1+2y)\sqrt{\zeta}}(2 + h_1(-1 + \zeta)\sqrt{\zeta} - h_2(-1 + \zeta)\sqrt{\zeta})^3 A_2 + 24e^{(h_1+2(h_2+y))\sqrt{\zeta}}(2 + \\ & h_1(-1 + \zeta)\sqrt{\zeta} - h_2(-1 + \zeta)\sqrt{\zeta})(2 - h_1(-1 + \zeta)\sqrt{\zeta} + h_2(-1 + \zeta)\sqrt{\zeta})^2 A_2 \left. \right) \Big] / \left(8 \left(e^{h_2\sqrt{\zeta}}(-2 + \right. \right. \\ & \left. \left. h_1(-1 + \zeta)\sqrt{\zeta} - h_2(-1 + \zeta)\sqrt{\zeta}) + e^{h_1\sqrt{\zeta}}(2 + h_1(-1 + \zeta)\sqrt{\zeta} - h_2(-1 + \zeta)\sqrt{\zeta}) \right)^3 \zeta \right) + A_3 + yA_4 \tag{5.14} \end{aligned}$$

We shall mention the functions (c1,c2,c3,c4,A1,A2,A3,A4) in the Appendix because they are huge expressions. The Eq.(4.20) can be written as

$$\frac{\partial p}{\partial x} = \Psi_{0_{yyy}} - \eta A \frac{\partial}{\partial y} \psi_{0_{yy}}^3 - \xi \Psi_{0_y} + A \Psi_{1_{yyy}} - \eta A^2 \frac{\partial}{\partial y} \Psi_{1_{yy}}^3 - \xi A \Psi_{1_y} \tag{5.15}$$

The pressure rise per wave length (Δp) is defined as

$$\Delta p = \int_0^1 \frac{\partial p}{\partial x} dx. \tag{5.16}$$

6 The Energy equation’s Solution

We get at this conclusion after The problem was solved using the approximation with a long wavelength and a low Reynolds number Eq.(4.22):

$$\frac{1}{Pr} \left(\frac{\partial^2}{\partial y^2} \theta \right) + Ec \left(\frac{\partial^2 \Psi}{\partial y^2} \right)^2 = 0. \tag{6.1}$$

The solution of equation (6.1) with boundary conditions

$$\theta = 0 \text{ at } y = h_1 \text{ and } \theta = 1 \text{ at } y = h_2. \tag{6.2}$$

After substituting into equation (6.1), and using boundary conditions (6.2), the constants r1 and r2 are determined.

7 Results and Discussion

To study the effect of physical parameters such as Effect of Hartman number (Ha), Darcy number (Da), material fluid (A), inclination of magnetic field (β), porous medium parameter w and amplitude ratio (\emptyset), we have plotted pressure gradient (dp/dx), pressure rise (Δp) and temperature (θ) in figs. 2.-20. are illustrated using the software MATHEMATICA.

7.1 Pressure Gradient dp/dx

The impact of important parameters on pressure gradient dp/dx can be shown graphically through figs. 2-7. Figs. 2. , 5. that ascending values of Hartman number Ha and the material fluid A lead to the pressure gradient decreases . In Figs 3., 4. the pressure gradient increases with increase of Da, β and then gradually disappeared as there is no effect on axial Pressure Gradient close the right, and left wall of the channel. We notice, the pressure gradient increases with the increase of w as displayed in fig 6. Fig. 7 shows the effect of \emptyset on the axial Pressure Gradient dp/dx . It is remarkable, that the increasing in \emptyset lead to dp/dx increase at the channel left wall, while dp/dx then gradually disappeared as there is no effect on axial Pressure Gradient close to the channel right wall.

7.2 Pressure Rise Δp

The rising of different pressure in Figures can be remarked in 8-13 in wave outline capacity of volumetric stream rate for various Hartmann numbers Ha , material fluid A , Darcy number Da , porous medium parameter w , inclination of magnetic field β , and amplitude ratio \emptyset . In this part, we demonstrate the relationship between the average pressure of non-dimensional rises for each wave length, and the dimensionless means flow rate $Q1$ and fluctuation in as an important factors included in p . The p expression finally can be found by In Mathematica, Im running a rmmmerical integration d/dx of a series approximation. A linear relationship between flow rate and p is depicted by plots., as well as the four partitions can be remarked when they are separated from the pumping zone. Peristaltic pumping can be presented in positive pumping with ($\Delta p > 0, Q1 > 0$). The co-pumping region or what they call it augmented flow is known as the second zone, and it is responsible for ($\Delta p < 0, Q1 < 0$). The third zone with no flow is recognized when ($\Delta p < 0, Q1 < 0$), and when ($\Delta p = 0$) the free pumping region is obtained. corresponds to the free pumping region. The pressure rise p increases as the Hartmarm rmmber Ha grows, as shown in Fig.8. the pumping rate drops in a cop urging zone where ($\Delta p < 0, Q1 < 0$) with a rise in As shown in the graph, Ha is rising in a retrograde zone ($\Delta p > 0, Q1 > 0$), The pressure rise p decreases with increasing phase difference Da, β and w , as seen in Figs 9.10., and 12 . Pumping is shown to increase in the increased pumping and cop-mmping regions ($\Delta p < 0$). Figure 11 demonstrates that as the material fluid A is increased, the pressure rise p decreases. In a retrograde region, as seen in the graph, ($\Delta p > 0, Q1 > 0$) and ($\Delta p < 0, Q1 < 0$) are both present. In all three areas, we found that p decreases as material fluid A increases (retrograde purming, co-pumping and augmented pumping regions) Fig.13 indicates that as the amplitude ratio increases, the pressure rise p increases. In a retrograde zone, ($\Delta p > 0, Q1 > 0$) and ($\Delta p < 0, Q1 < 0$) can be seen on the graph.

7.3 Temperature distribution θ

The temperature field influences several factors, including the Prandtl number Pr, Hartman number Ha, eckert number Ec, Darcy number Da, material fluid A, magnetic field inclination, porous media parameter w , and amplitude ratio shown in Figures 14-21. In Figs 14, 15 and 16 shows that the temperature field with increasing Pr, Ec and Ha no change in the channel central region, while the temperature field increases near from the channel wall boundary. Figs 17 and 20 shows that the temperature field with increasing Da and w no change in the central region of the channel, while the temperature field decreases in near from the boundary of the channel wall . Fig 18 shows that the temperature field with increasing β no change in the central region and left of the channel, while the temperature field decreasing in near from the boundary right of the channel wall .From fig 19. noted that the temperature field do not change at increasing in A . Fig. 21 shows that the temperature field with increasing \emptyset has no change in the central region and right of the channel, while the temperature field increases near from the left channel wall boundary.

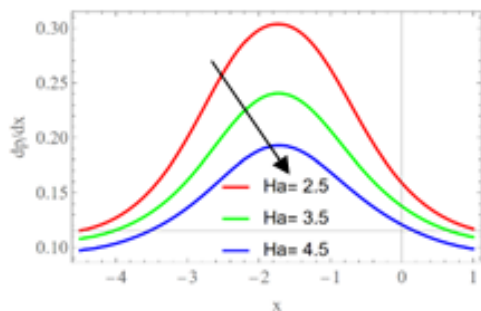


figure 2. pressure gradient's variation for different values of Ha when $Da = 0.2, \beta = 0.1, A = 0.2, w = 0.1, Q = 1.5, \theta = 0.2, a = 0.2, b = 0.2, d^* = 0.5$

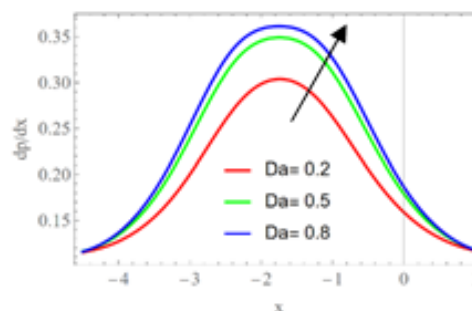


figure 3. Pressure gradient's variation for different values of Da when $Ha = 2.5, \beta = 0.1, A = 0.2, w = 0.1, Q = 1.5, \theta = 0.2, a = 0.2, b = 0.2, d^* = 0.5$

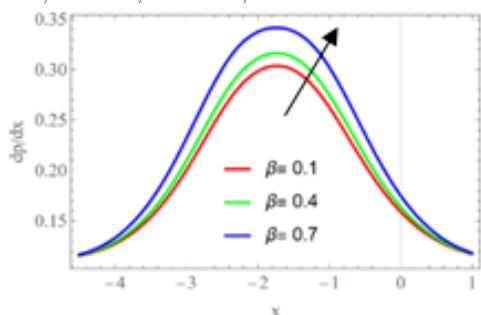


figure 4. Pressure gradient's variation for different values of β when $Ha = 2.5, Da = 0.2, A = 0.2, w = 0.1, Q = 1.5, \theta = 0.2, a = 0.2, b = 0.2, d^* = 0.5$

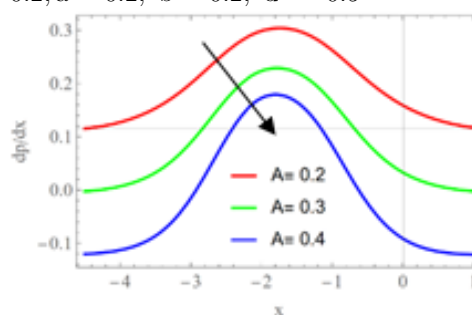


figure 5. Pressure gradient's variation for different values of A when $Ha = 2.5, Da = 0.2, \beta = 0.1, w = 0.1, Q = 1.5, \theta = 0.2, a = 0.2, b = 0.2, d^* = 0.5$

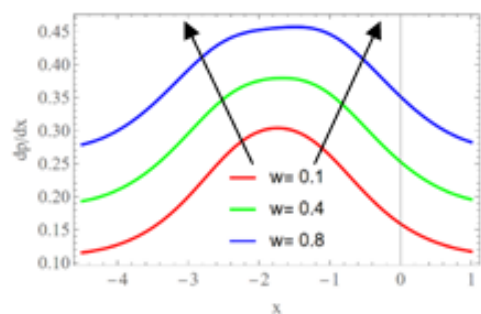


figure 6. Pressure gradient's variation for different values of w when $Ha = 2.5, Da = 0.2, \beta = 0.1, A = 0.2, Q = 1.5, \theta = 0.2, a = 0.2, b = 0.2, d^* = 0.5$

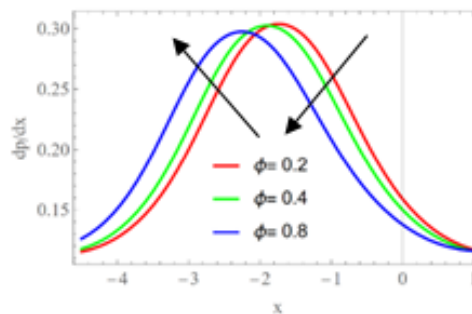


figure 7. Pressure gradient's variation for different values of θ when $Ha = 2.5, Da = 0.2, \beta = 0.1, A = 0.2, Q = 1.5, w = 0.1, a = 0.2, b = 0.2, d^* = 0.5$

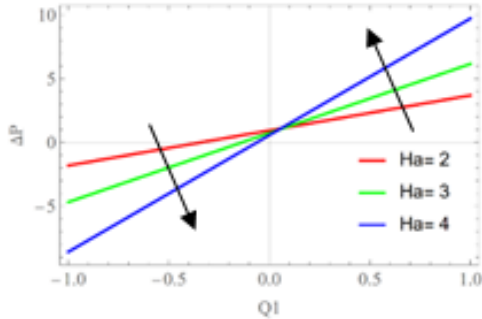


Figure 8. Pressure's variation rise ΔP with $Q1$ for different values of Ha when $Da = 0.9, \beta = 0.2, A = 0.1, w = 0.8, Q = 1.5, \phi = 0.2, a = 0.2, b = 0.2, d^* = 0.5$

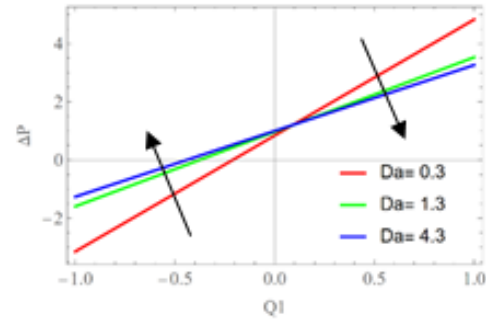


Figure 9. Pressure's variation rise ΔP with $Q1$ for different values of Da when $Ha = 2, \beta = 0.2, A = 0.1, w = 0.8, Q = 1.5, \phi = 0.2, a = 0.2, b = 0.2, d^* = 0.5$

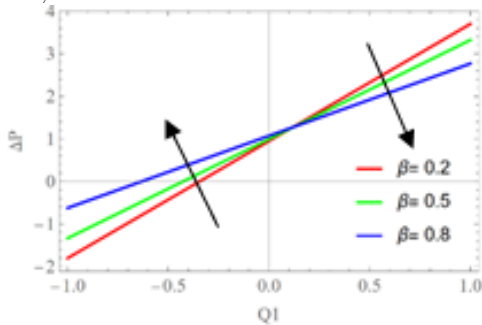


Figure 10. Pressure's variation rise ΔP with $Q1$ for different values of β when $Ha = 2, Da = 0.9, A = 0.1, w = 0.8, Q = 1.5, \phi = 0.2, a = 0.2, b = 0.2, d^* = 0.5$

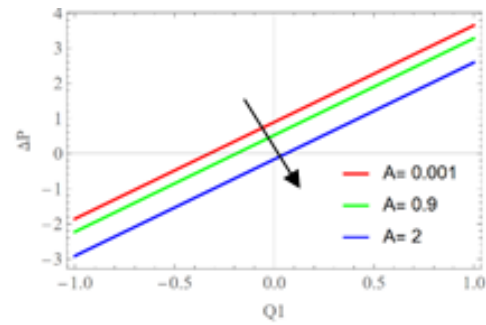


Figure 11. Pressure's variation rise ΔP with $Q1$ for different values of A when $Ha = 2, Da = 0.9, \beta = 0.2, w = 0.8, Q = 1.5, \phi = 0.2, a = 0.2, b = 0.2, d^* = 0.5$

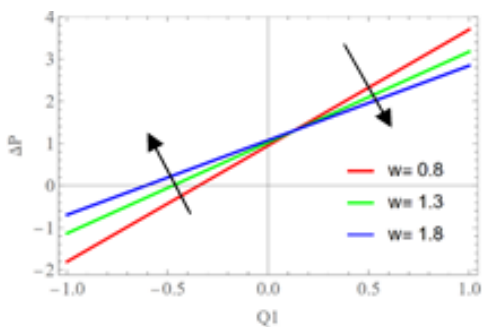


Figure 12. Variation of pressure rise ΔP with $Q1$ for different values of w when $Ha = 2, Da = 0.9, \beta = 0.2, A = 0.1, Q = 1.5, \phi = 0.2, a = 0.2, b = 0.2, d^* = 0.5$

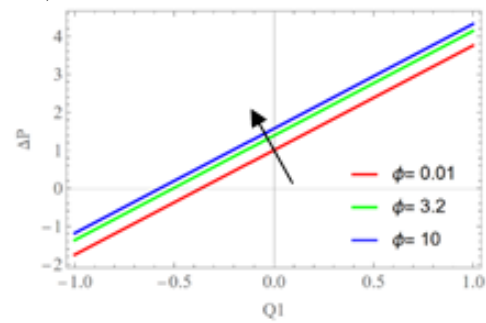


Figure 13. Pressure's variation rise ΔP with $Q1$ for different values of ϕ when $Ha = 2, Da = 0.9, \beta = 0.2, A = 0.1, w = 0.8, Q = 1.5, a = 0.2, b = 0.2, d^* = 0.5$

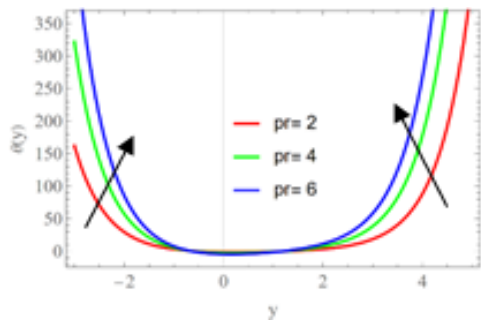


Figure 14. temperature's variation of θ with y for different value of Pr at $Ha = 1.5, Da = 1, \beta = 0.1, A = 0.3, w = 0.3, Q = 0.5, \theta = 0.3, d^* = 0.5, Ec = 3, a = 0.2, b = 0.2$

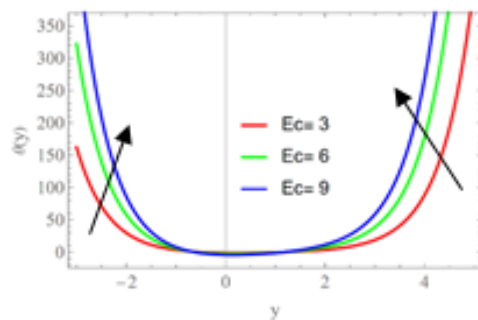


Figure 15. temperature's variation of θ with y for different value of Ec at $Ha = 1.5, Da = 1, \beta = 0.1, A = 0.3, w = 0.3, Q = 0.5, \theta = 0.3, d^* = 0.5, Pr = 2, a = 0.2, b = 0.2$

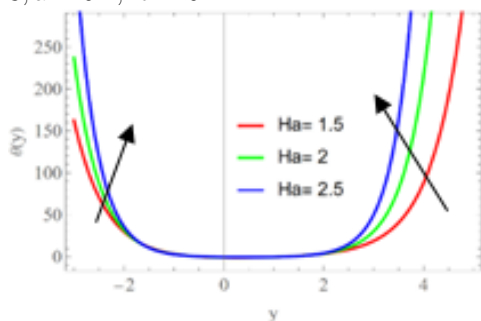


Figure 16. temperature's variation of θ with y for different value of Ha at $Da = 1, \beta = 0.1, A = 0.3, w = 0.3, Q = 0.5, \theta = 0.3, d^* = 0.5, Pr = 2, Ec = 3, a = 0.2, b = 0.2$

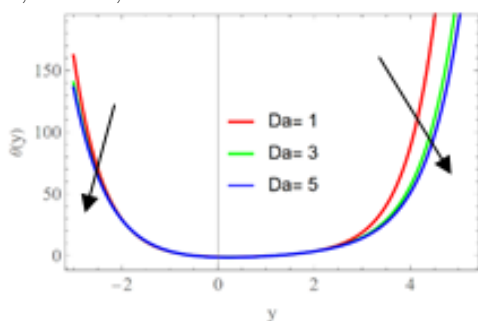


Figure 17. temperature's variation of θ with y for different value of Da at $Ha = 1.5, \beta = 0.1, A = 0.3, w = 0.3, Q = 0.5, \theta = 0.3, d^* = 0.5, Pr = 2, Ec = 3, a = 0.2, b = 0.2$

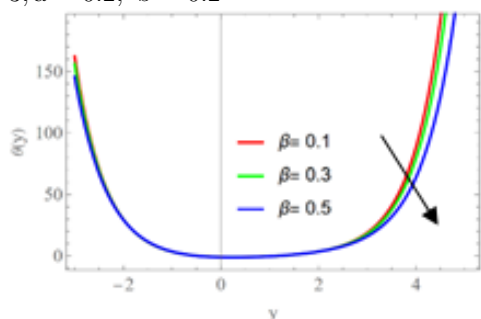


Figure 18. temperature's variation of θ with y for different value of β at $Ha = 1.5, Da = 1, A = 0.3, w = 0.3, Q = 0.5, \theta = 0.3, d^* = 0.5, Pr = 2, Ec = 3, a = 0.2, b = 0.2$

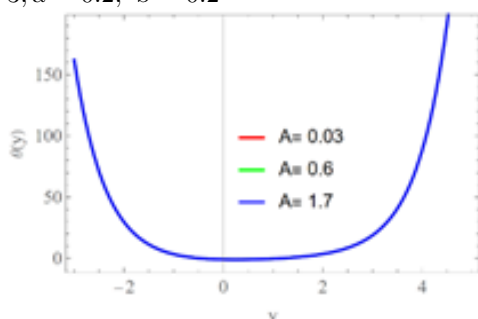


Figure 19. temperature's variation of θ with y for different value of A at $Ha = 1.5, Da = 1, \beta = 0.1, w = 0.3, Q = 0.5, \theta = 0.3, d^* = 0.5, Pr = 2, Ec = 3, a = 0.2, b = 0.2$

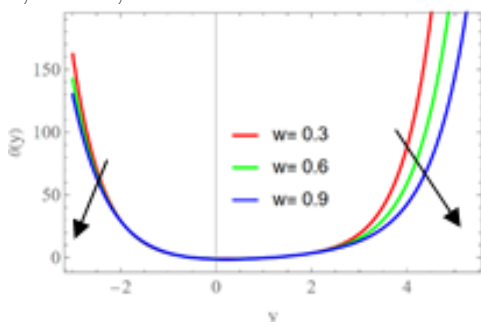


Figure 20. temperature's variation of θ with y for different value of w at $Ha = 1.5, Da = 1, \beta = 0.1, A = 0.3, Q = 0.5, \theta = 0.3, d^* = 0.5, Pr = 2, Ec = 3, a = 0.2, b = 0.2$

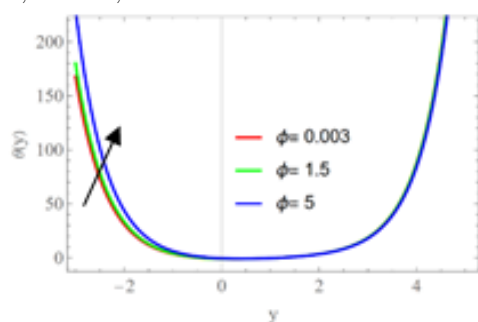


Figure 21. temperature's variation of θ with y for different value of θ at $Ha = 1.5, Da = 1, \beta = 0.1, A = 0.3, w = 0.3, Q = 0.5, d^* = 0.5, Pr = 2, Ec = 3, a = 0.2, b = 0.2$

8 Conclusion

Considering the current study, some of the interesting conclusions were summarized and special emphasis has been paid to study Influence of Inclined Magnetic Field and Heat Transfer on Peristaltic Transfer Powell-Eyring Fluid in Asymmetric Channel and Porous Medium. The results are discussed can be seen hereunder :

- The influence of relevant parameters on pumping rate vary depending on the pumping region.
- The temperature increases near the channel wall of the boundary with increasing Ha , Pr and Ec , with no change in the channel central region. The temperature decreases in near from the boundary of the channel wall with increasing Da and w , without any change in the channel of central .
- There is no change in temperature field at increasing in A and \emptyset . Also, there is no change in the central region and the right of the channel, while the temperature field increasing in near from the boundary left of the channel wall and the increasing in β no change in the central region and left of the channel, while the temperature field increasing in near from the right of the channel walls' boundary.

References

- [1] M. Abbas and M. Bhatti, *Simultaneous effect of slip and MHD on peristaltic blood flow of Jeffrey fluid model through a porous medium*, Alexandria Engin. J. **55** (2016), 1017–1023.
- [2] F. Abbasi, T. Hayat and B. Ahmad, *Hydromagnetic peristaltic transport of variable viscosity fluid with heat transfer and porous medium*, Appl. Math. Inf. Sci. **10** (2016), 2173–2181.
- [3] H.A. Ali and A.M. Abdilhadi, *The peristaltic transport of MHD Powell-Eyring fluid through porous medium in asymmetric channel with slip condition*, Int. J. Sci. Res. **6** (2016), no. 12.
- [4] M. Devakar, K. Ramesh, S. Chouhan and A. Raje, *Fully developed flow of non-Newtonian fluids in a straight uniform square duct through porous medium*, J. Assoc. Arab Univ. Basic Appl. Sci. **23** (2017), 66–74.
- [5] T. Hayat, Q. Hussain and N. Ali, *Influence of partial slip on the peristaltic flow in a porous medium*, Physica A **387** (2008), 3399–3409.
- [6] T. Hayat, S. Shah, B. Ahmad, M. Mustafa, *Effect of slip on peristaltic flow of Powell-Eyring fluid in a symmetric channel*, Appl. Bionics Biomech. **11** (2014), 69–79.
- [7] S. Hina, *MHD peristaltic transport of Eyring-Powell fluid with heat/mass transfer, wall properties and slip conditions*, J. Magnetism Magnetic Materials **404** (2016), 148–158.
- [8] G. Ismail, F. Darwesh and N. Dabe, *Peristaltic transport of a magneto non-Newtonian fluid through a porous medium in a horizontal finite channel*, IOSR J. Math. **8** (2013), 32–39.
- [9] R.C. Kenneth and P. Shih, *Magneto fluid dynamics for engineers and applied physicists*, Scripta Publishing Company, 1973.
- [10] A. Khan, R. Ellahi and M. Usman, *The effects of variable viscosity on the peristaltic flow of non-Newtonian fluid through a porous medium in an inclined channel with slip boundary conditions*, J. Porous Media **16** (2013), no. 1.
- [11] T.W. Latham, *Fluid motion in a peristaltic pump*, M. S. Thesis, Massachusetts Institute of Technology, Cambridge, 1966.
- [12] F. Oyelami and M. Dada, *Transient magnetohydrodynamic flow of Eyring-Powell fluid in a porous medium*, Ife J. Sci. **18** (2016), no. 2.
- [13] A.H. Shapiro, M.Y. Jaffrin and S.L. Wienberg *Peristaltic pumping with long wavelengths at low Reynolds number*, J. Fluid Mech. **37** (1969), 799–825.
- [14] A. Tanveer, A. Alsaedi, M. Shafique, T. Hayat, *Magnetohydrodynamic effects on peristaltic flow of hyperbolic tangent nanofluid with slip conditions and joule heating in an inclined channel*, Int. J. Heat Mass Transfer **102** (2016), 54–63.
- [15] M. Veerakrishna and B. Swarnalathamma, *Convective heat and mass transfer on MHD peristaltic flow of Williamson fluid with the effect of inclined magnetic field*, Int. Conf. Condensed Matter Appl. Phys. 2015, 020461-1-020461-8.